Persistent effects of pair bonding in lung cancer cell growth in monogamous Peromyscus californicus

Asieh Naderi[1]; Elham Soltanmohammadi[1]; Vimala Kaza[2]; Shayne Barlow[3]; Ioulia Chatzistamou,[4] & Hippokratis Kiaris[1,2]*

[1]Department of Drug Discovery and Biomedical Sciences, College of Pharmacy, University of South Carolina, SC, USA

[2]Peromyscus Genetic Stock Center, University of South Carolina, SC, USA

[3]Department of Cell Biology and Anatomy, School of Medicine, and Animal Resources Facility, University of South Carolina, SC, USA

[4]Department of Pathology, Microbiology and Immunology, School of Medicine, University of South Carolina, SC, USA.

Keywords: Cancer, widowhood, tumor spheroids, cancer stem cells, hierarchical clustering

***Correspondence**: Hippokratis Kiaris Ph.D., CLS 713, 715 Sumter St., Columbia, SC 29208-3402 Phone: 803 3611 781 Email: hk@sc.edu

Abstract

Epidemiological evidence suggests that social interactions and especially bonding between couples influence tumorigenesis, yet whether this is due to lifestyle changes, homogamy (likelihood of individuals to marry people of similar health), or directly associated with host-induced effects in tumors remains debatable. In the present study, we explored if tumorigenesis is associated with the bonding experience in monogamous rodents at which disruption of pair bonds is linked to anxiety and stress. Comparison of lung cancer cell spheroids that formed in the presence of sera from bonded and bond-disrupted deer mice showed that in monogamous P. polionotus and P. californicus, but not in polygamous P. maniculatus, the disruption of pair bonds altered the size and morphology of spheroids in a manner that is consistent with the acquisition of increased oncogenic potential. In vivo, consecutive transplantation of human lung cancer cells between *P. californicus,* differing in bonding experiences (n=9 for bonded and n=7 for bond-disrupted), and nude mice showed that bonding suppressed tumorigenicity in nude mice ($P<0.05$), suggesting that the protective effects of pair bonds persisted even after bonding ceased. Unsupervised hierarchical clustering indicated that the transcriptomes of lung cancer cells clustered according to the serum donors' bonding history while differential gene expression analysis pointed to changes in cell adhesion and migration. The results highlight the prooncogenic effects of pair-bond disruption, point to the acquisition of expression signatures in cancer cells that are relevant to the bonding experiences of serum donors and question the ability of conventional mouse models to capture the whole spectrum of the impact of the host in tumorigenesis.

Introduction

While the psychosomatic impact of cancer in patients is extensively documented, the reciprocal effects of individuals' social experiences in carcinogenesis receive limited attention. Both anecdotal and experiential evidence, as well as numerous epidemiological studies, strongly suggest that emotional factors can affect the development and progression of cancer, pointing to the sensitivity of cancer cells to signals associated with behavior, emotional state, and sociality. For example, the marital status modulates the likelihood for the development of fatal cancers, with unmarried, divorced, or widowed individuals exhibiting an increased chance of developing life-threatening disease and males being more susceptible than females to the protective effects of marriage (1). The "widowhood effect" provides an example at which in couples, after the loss of one partner, the surviving one exhibits an increased probability for the development of various fatal pathologies (2-6). Notwithstanding that high variation in death causes has been documented, cancer is recognized as a common cause of mortality (1-3,7-9). Although both sexes are influenced by widowhood, males appear more sensitive than females to widowhood-associated death (10,11).

Despite the information they provide, unavoidable changes in lifestyle habits in the bereaved partner at widowhood or between single and married patients complicate the epidemiological data interpretation. Several mechanisms connecting cancer to social interactions, mental state, and bereavement have been proposed. Laboratory mice of the genus Mus, despite their power in illuminating various aspects of tumorigenesis, remain of limited value in modeling the effects of pair-bonding. It is estimated that in less than 10% of mammals, including humans, individuals form pair bonds that are based on mating (12-14). Therefore, mice, by not developing long-term pair bonds, are not adequate in studying the effects of widowhood and pair bond disruption (15,16). Earlier studies in mice have shown that brain-derived signals linked to the

reward system may impact tumorigenesis, whereas stress can stimulate metastases (17,18). However, more complex behavioral traits involving social interactions in married couples or widowhood cannot be studied in mice. Peromyscus californicus is a monogamous species developing long-term, cohesive pair bonds that can influence various physiological responses (19-21). Upon cyclosporine-mediated immunosuppression, similarly with other rodents, P. californicus supports the growth of human cancers, providing a potentially informative animal model for the study of pair-bond disruption in tumorigenesis in vivo (22-25).

Results

Bonding history modulates the effects of sera in tumor spheroid formation. Initially, we asked if sera of *P. californicus* following the disruption of pair bonds affected the growth of cancer cells *in vitro* in a manner that depended on bonding history. We focused on the formation of tumor spheroids that are enriched in cells with cancer stem cell (CSC)-like properties, and their formation is known to reflect tumorigenic activity directly (26, 27). Sera were obtained from 14-17 months old virgin, bonded for about 12 months, or bond-disrupted (after 12 months of bonding) at the periods indicated, male *P. californicus,* and the efficacy of spheroid formation by A549 human lung cancer cells was assessed. A pilot study indicated that sera obtained from animals 1 week after the disruption of pair bonds resulted in the formation of larger yet less compact spheroids, suggesting a significant impact of bond disruption in spheroid morphogenesis (Fig. 1a). The results were confirmed and extended in a subsequent study that also included sera obtained 24h and 2 weeks after the disruption of pair bonds(Fig. 1b). In this study, sera from 9 (B), 5 (BD, 24h), 5 (BD, 1wk), 4 (BD, 2wk), and 5 (V) different animals were used, and microsphere formation was evaluated in 2 biological replicas for each (n=10 for BD (1wk), BD (24h) and v; n=8 for BD (2wks) and n=18 for B). For control media (CM) and plain serum-free media (PM) n=4. As shown in Fig.

1b, this activity was only marginal at 24h but was significant ($P<0.05$) 1 week and 2 weeks after the disruption of pair bonds, implying that the factors responsible accumulated in the sera after pair-bond disruption. As compared to virgins, sera from animals at bonding resulted in the formation of smaller spheroids, albeit insignificantly, which implies that bonding may also have some protective activity, beyond the prooncogenic activity of bond disruption (Fig. 1b).

Variation in spheroid size with sera obtained after bond disruption is due to the genetic diversity of donor animals and persists in different lung cancer cell lines. The effects in spheroid size described above were obtained with sera from older animals (14-17 months old) that were bonded for at least 12 months. To test if disruption of bonds in younger animals that were bonded for shorter time periods also produced similar effects, we conducted the following study: We exposed to sera of 8-10 months old animals that were either pair-bonded for 2 months or following 2 weeks of bond disruption after 2 months of bonding, a roster of lung cancer cell lines. For this experiment 14 animals were used that represented 7 sibling pairs with each sibling allocated either to the bonded or to the bond-disrupted group. Our results indicated that consistently, in the same sibling pair, an induction of microsphere size of similar magnitude was noted for all 5 cell lines tested, in 4 out of 7 pairs, while this effect was only marginal in the remaining 3 pairs (Figure 1-Figure Supplement 1). The variation in spheroid size was analogous to that recorded in the results described in Figure 1c. Thus, we conclude that even shorter periods of bonding are sufficient, and the consequences of its disruption can be recorded in sera from even younger animals. More importantly it indicates that the variation of the effects is due to the diversity of the animals and not to the differential sensitivity of the cell lines used.

Persistent pro-oncogenic activity of bond disruption in vivo. The effects of pair-bonding in spheroid formation prompted us to explore if bond-disruption also influences the efficacy of

tumorigenesis in vivo. To that end, vasectomized male *P. californicus* were allowed to establish pair bonds for about 2 months with their female partners and then subjected to pair bond disruption (n=9) or were left with their partners (n=11). Following immunosuppression by CsA animals were inoculated with A549 human lung cancer cells and tumorigenesis was monitored. Animals that did not possess bonding experiences before were used as controls (n=8). Tumors grew originally in animals of all experimental groups and by day 15 measurable tumors were detected in 9 out of 11 bonded, in 8 out of 9 bond-disrupted and in 6 out of 8 virgins (Fig. 2a). At this point, tumors were modestly - albeit not statistically significantly - larger in the bond-disrupted animals and smaller in the group of virgins (Fig. 2a). By day 25, the tumors persisted in both the bond-disrupted and bonded animals, at 89% (8 out of 9) and 82% (9 out of 11) rate respectively, while in virgin animals, they were detectable only in 25% (2 out of 8) of the animals (Fig. 2b,c).

In a follow-up study we explored if differential prooncogenic activity persisted after growth in nude mice. Thus, tumors that were originally grown in *P. californicus* for at least one month (n=9 for bonded and n=7 for bond-disrupted), were re-transplanted in virgin nude mice (1 nude mice for each original Peromyscus tumor) and tumorigenesis was recorded. As shown in Figure 2d, tumors from bonded *P. californicus* exhibited significantly (P=0.011) lower tumorigenicity in nude mice than those grown originally in the bond-disrupted animals, despite that histologically they remained indistinguishable (Fig. 2e). In line with the tumor spheroid analyses, pair-bonding produced persistent changes in tumors that suppressed their growth and endured even when bonding seized.

Effects of pair bonding in differential gene expression. The effects of bonding history in the profile of tumor growth *in vivo,* combined with the spheroid formation *in vitro,* implies the induction of transcriptional changes in the cancer cells in a manner that depends on bonding

experience (Figure 3 and Figure 3- Figure Supplement 1, 2 and 3). Initially, we focused on the expression of established CSC markers and genes regulating CSC potential, such as Oct-4, b-catenin, and CD-133 that have been identified previously in A549 cells (28-30). The analysis was performed by semiquantitative RT-PCR in 2D-cultures to eliminate the effects of the clonal selection of cells in the spheroids. Differential expression analysis did not reveal considerable differences between the bonding groups, either in cells cultured in vitro with sera from animals differing in bonding history or in vivo in tumors in nude mice or Peromyscus (Figure 3- Figure Supplement 1). However, unsupervised hierarchical clustering indicated that these CSC markers provided a signature that predicted a relatively high accuracy bonding history of the animals (Figure 3- Figure Supplement 1).

This observation prompted us to perform RNA sequencing and analyze expression profiles at the whole transcriptome level in human A549 lung cancer cells in the presence of sera that had been isolated from monogamous male P. californicus that were virgin (V), bonded (B), or subjected to disruption of pair bonds (BD) after bonding (n=6 samples/group). Controls (C) cultured in the presence of FBS were also included. Unsupervised hierarchical clustering (31) indicated that the transcriptomes clustered well together according to the serum donors' bonding history, except the virgin (V) group that exhibited the lowest discrimination (Figure 3- Figure Supplement 2). Differential gene expression analysis was performed as described before by using the iDEP platform (32). This analysis showed that the majority of differentially expressed genes were detected in the comparisons involving the FBS treated cells (C) which suggests that the species origin of sera produces the most potent effects in gene expression and potentially masking the consequences of pair bonding in the regulation of the transcriptome (Figure 3- Figure Supplement 3). Thus, we repeated the analysis by excluding the specimens corresponding to FBS

and restricted it only to the specimens that received Peromyscus sera (Figure 3). Seven genes were differentially expressed in each B vs BD and B vs V comparisons, while none were detected between the V and BD groups (Table 1). Thus, it seems that pair-bonding produces more robust effects in the sera as compared to those of bond disruption. Among these genes, all of which were downregulated in the B group, 5 were common and included HES1, ZFP36, NR4A1, FGG, and SOCS3. Hes1 is a transcription factor that is downstream of Notch signaling, for which the prooncogenic activity in lung cancer has been established (33,34). NR4A1 encodes for the orphan nuclear receptor A1 for which a strong association with unfavorable outcome in lung cancer has been shown and is involved in cancer cell migration (35,36). SOCS3 is a suppressor of cytokine signaling and is a repressor of lung tumorigenesis (37,38). FGG encodes for fibrinogen gamma chain that has been linked to enhanced invasion of lung and other cancer cells (39,40). The genes that were uniquely detected in the BD vs B groups comparison were FGA and FGB, which encode for fibrinogen A and B chains (41) while in the V vs B comparison, the oncogene Jun that enhances lung cancer cell migration (42) and the connective tissue growth factor (CTFG) that at least in lung cancer, is associated with favorable prognosis (43,44). Pathway enrichment analysis indicated that processes associated with differentially expressed genes were linked to the regulation of cell migration and spread, or tissue morphogenesis (Table 2).

Monogamous and not polygamous Peromyscus are sensitive to the effects of bond disruption in spheroid formation. The findings on P. californicus prompted us to explore if other Peromyscus species are also sensitive to the effects of the disruption of pair bonds. Thus, we compared the effects of sera from bonded or bond-disrupted polygamous P. maniculatus and monogamous P. polionotus, in the size and shape of A549 tumor spheroids. As shown in Figure 4, the disruption of pair bonds altered spheroid morphology in the monogamous but not in the

polygamous species. The intensity of this effect was variable among the animals tested and was recorded in at least 6 out of 12 male P. polionotus but none of P. maniculatus (n=12) tested (P=0.005, chi-square test; Figure 4- Figure Supplement 1). Contrary to P. californicus though, at which pair bond disruption enhanced spheroid size, in P. polionotus the primary effect was seen in the spheroids' shape: Spheroids that formed in the presence of P. polionotus sera obtained after the disruption of pair bonds had scattered morphology, as opposed to the spheroids from P. maniculatus sera at bonding and bond disruption and those of P. polionotus at bonding that were smooth-edged. In some instances (about 25% of animals), this scattered phenotype was also noted in P. polionotus sera obtained at bonding (Figure 4- Figure Supplement 1). Whether this difference represents the actual phenotypic difference between the two species or is due to methodological changes in the state of the cells and donor animals remains to be established. In addition, it may reflect the same effect (cell dispersion followed by proliferation) but recorded at different stages during the formation of the spheroids. It is also noted, that the monogamous behavior in Peromyscus has developed independently during the evolution of P. polionotus and P. californicus, and thus alternative signaling ques may have been engaged in altering the consequences of bond disruption in spheroid formation (45). To that end, the signaling cascades influencing spheroid size and shape may be distinct for the two species; nevertheless, the effects of pair-bond disruption persist.

Discussion

The present findings exemplify the role of the context - in its wider sense - in cancer progression and underscore the significance of psychosomatic factors as modulators of cancer growth. Using a behaviorally relevant animal model, our results highlight the biological basis of the "widowhood

effects" and suggest that it operates as a tumor-promoting factor, beyond lifestyle changes. Our conclusions are based on the recorded effects of pair bonding in three major phenotypic characteristics of the cancer cells. Those included tumor spheroid formation established in the presence of sera from bond-disrupted animals, the expression profile of the cancer cells in vitro and in vivo that depended on the bonding history of serum donors and tumor hosts, respectively, and ultimately their tumorigenicity in the nude mice. The use of sera from outbred, genetically diverse rodents, allowed us to obtain evidence that this effect varies among individuals but persists across different lung cancer cells. This observation might be of relevance to the study of human populations that are genetically diverse and their responses to the same stimuli may be variable.

In our animal model, cancer cells were implanted in tumor-free animals and the kinetics of tumorigenesis was affected by the animals' bonding history. Whether pair bonding and disruption can also influence tumor initiation will have to be established, nevertheless, the fact that most cancers are slow growing in patients is consistent with the effects of widowhood in influencing the progression, as opposed to the initiation of the disease. Yet, by using for the in vivo experiments immunocompromised animals (nude mice and cyclosporine administration), our study suffers from the absence of integration of immune responses that may be especially relevant to widowhood-associated stress.

An unexpected finding was the loss of the tumors in the virgin animals as opposed to the majority of the bonded and bond-disrupted that retained them (Figure 2b). A possible explanation is probably related to the differential effectiveness of immunosuppression by cyclosporine. Especially during the initial period after cancer cell inoculation, cyclosporine may have caused more potently immunosuppression in the animals that had been subjected to bonding, due to the concomitant anti-inflammatory action of oxytocin, a neurohormone with essential role in the

establishment of social interactions and pair bonding (46-50). It is noted though that the high difference in the tumorigenicity between virgins and the bonded or bond-disrupted animals, renders differential immune suppression unlikely as the sole contributor for this discrepancy.

Differential analysis of gene expression showed that sera from animals at bonding, enriched for genes regulating cell migration and spreading, and tissue morphogenesis, features that are consistent with the recorded changes in spheroid morphology. Although for several of the differentially expressed genes, their downregulation, which was seen in the bonded group, was associated with a favorable prognosis, in some cases, it wasn't. For example, SOCS3 was downregulated in the bonding group, yet it is a tumor suppressor for lung and other cancers (37,38), which may reflect responses related to oxytocin signaling during bonding (51).

Beyond its effects in the expression of individual genes, the impact of bonding history in transcription was more clearly reflected in the similarity recorded in the transcriptomic profiles of cells cultured in sera from animals with similar bonding experiences. This was especially pertinent to the bonded and bond-disrupted groups. An intriguing possibility is that this is indicative for the lowest rigidity in the transcriptomic profile induced by the serum of virgin animals, as opposed to the changes triggered by the sera of bonded and of bond-disrupted animals that remained more robust.

Collectively the results provide a mechanistic foundation for the widowhood effect and suggest that the individuals' social, and especially bonding experiences, modify the transcriptome of lung tumors modulating oncogenic activity. As such, they advocate that cancers at widowhood represent a distinct pathological entity that may deserve targeted therapeutic strategies, which should take into consideration social interactions. Thus, preventive measures could be developed to mitigate such pro-oncogenic effects in individuals at bereavement. Whether these findings do

occur and at which extent in other monogamous species, including humans, and if they are applicable to other cancers as well as other pathologies beyond malignancy, remains to be explored. Finally, the present results also raise some concerns regarding the use of conventional animal models and their ability to accurately capture the whole spectrum of the tumorigenic process and the associated host-derived factors.

Methods and Materials

Animal studies. Genetically diverse male *P. californicus* (stock IS), P. polionotus (PO stock), and P. maniculatus (BW stock) were obtained from the Peromyscus Genetic Stock Center (Columbia, SC) (RRID:SCR_002769). Mice were all 14-17 months old and were divided into three experimental groups: bonded, bond-disrupted, and virgin. For the tumor inoculation studies, in the bonded group, mice were paired for at least 2 months before the study began and remained paired until the end of the study. In the bond-disrupted group, mice were paired 2 months before the study started, and immediately after cancer cells injection, they were separated. In the virgin group, mice were kept individually 2 months before the study began. Vasectomy was performed to prevent pregnancy during the study. Some siblings were used and were distributed randomly in different experimental groups as described in the legend of Figure 1-Figure Supplement 1. Nude mice (male, 6-8 weeks old) were obtained from Charles River Laboratories (Boston, MA) and were housed in groups of 4-5. For serum collection used in the RNAseq studies and spheroid formation, for the bonded group, mice were paired for about 12 months. For the bond-disrupted group, we separated paired mice after 12 months of bonding and collected the sera one week after bond-disruption. For virgin mice, we collected sera from mice housed 3/cage. Sera were obtained by retro-orbital bleeding before and after bond disruption at the indicated times. Animal studies were approved by the University of South Carolina IACUC (Protocol # 2473-101464-102319).

Cell lines: A549 human non-small cell lung adenocarcinoma cells were originally obtained from ATCC (Manassas, VA) and thereafter maintained in freezing media (60% DMEM, 30% FBS, 10% DMSO). Most recently, cells were validated by STR typing (Biosynthesis, Lewisville, TX) just after completion of experiments. Human H1703 squamous, H596 adenosquamous, H358 bronchioalveolar, and H292 mucoepidermoid lung cancer cells were obtained prior to their use

from ATCC (Manassas, VA), and cultured for 3 passages at ATCC-recommended media prior to the performance of the spheroid assays. Cells were tested negative for mycoplasma contamination.

Tumor inoculation. To cause immunosuppression in *P. californicus* and overcome xenograft rejection, animals were treated daily with 100 mg/kg cyclosporine A (in 90% olive oil and 10% EtOH) s.c. starting one day before the implantation of cancer cells, for 2 weeks, and then every other day for the whole duration of the study (20). For cancer cell inoculation, (5×10^6) cells were injected subcutaneously into the right flank of mice in a total volume of 100 μl PBS. Tumor volumes were assessed by using the formula $(\text{width})^2 \times \text{length}/2$. All experiments were approved by the Institutional Animal Care and Use Committee of the University of South Carolina (approval no. 101464). For re-transplantation in nude mice, tumors were harvested from *P. californicus*, mechanically minced at pieces of 5-10 $mm^{3,}$ and were implanted into the right flank of nude mice using a trocar needle. Mice were followed up each week until four months.

Histology. Tumor was fixed in 4% neutral buffered formalin and subsequently embedded in paraffin. Sections were stained with Hematoxylin and Eosin (H&E) for histological assessment. Where available, a part of the tumor was snap-frozen on dry ice and stored at -80 ºC, for RNA extraction. Images were obtained by a Leica optical microscope.

Tumor spheroid formation. Lung cancer cells were seeded into 96-well spheroid microplates (Corning Cat. No. 4515) at 2×10^3 cells/well in 100 μL of Dulbecco's modified Eagle medium (DMEM) + 5% FBS + 5% serum of each mouse. The age of the mice, their bonding group and the period of bonding are described in the text and corresponding figure legends. The plate was incubated at 37°C, 5% CO2. Images were taken using an inverted microscope at 4X magnification each day until 3 days and analyzed using NIH ImageJ software to assess microsphere areas and volumes. The studies were repeated independently at least twice, and similar results were obtained.

For the assessment of the spheroids that formed with P. polionotus sera, “scattered” phenotype was scored when at least 2 outgrowths formed distal from the main spheroid.

Cell viability assay. Spheroid cell viability was assayed using the LIVE/DEAD™ Viability/Cytotoxicity Kit (Cat. No. L3224). After 3 days of spheroid culture, wells were rinsed 2 times with an 80 percent-volume change of media with D-PBS. EthD-1 (12 μM) and calcein AM (4 μM) were added to the wells, and the cells were incubated in the dark for 30-45 min to avoid the photodynamic effect. Images were taken using a fluorescence microscope; live cells fluoresce green, whereas dead cells fluoresce red. Data were analyzed using ImageJ image analysis software.

Quantitative Real-Time PCR analysis and RNA sequencing. Total RNA from cell and tumor tissues were isolated using the Qiagen RNeasy Mini Kit. Equal quantities of RNA were used for making cDNA using iScript cDNA synthesis kits (Bio-Rad) according to the supplier’s protocol on a T100 thermal cycler (Bio-Rad). Human-specific primers for cancer stem cell (CSCs) related genes; OCT4, β-catenin, and CD133 were designed using Primer3 and Primer BLAST. Quantitative Real-time PCR was performed using the Bio-Rad Real-Time PCR detection system and iTaq Universal SYBR Green Supermix (Bio-Rad) according to the manufacturer's instructions. Amounts of target genes mRNA were normalized to a reference gene GAPDH and were expressed as arbitrary units. The oligonucleotides used for qPCR amplification were: Oct-4: GAAGGATGTGGTCCGAGTGT (left) and GTGAAGTGAGGGCTCCCATA (right); b-catenin: GAAACGGCTTTCAGTTGAGC (left) and CTGGCCATATCCACCAGAGT (right); CD-133 TTGTGGCAAATCACCAGGTA (left) and TCAGATCTGTGAACGCCTTG (right); GAPDH: CCATCACCATCTTCCAGGAGCG (left) and AGAGATGATGACCCTTTTGGC (right). Hierarchical clustering analysis and presentation of expression data were performed using the Morpheus analysis software (https://software.broadinstitute.org/morpheus). For the analysis,

either raw cpm values were used or transformed by using the formula Log2 (1+raw values), as described in the text. RNA sequencing was performed as described (52). RNAseq data were deposited to NCBI (GSE167827). Differential analysis of gene expression and enrichment pathway analysis were performed by using the iDEP platform (37).

Statistical analysis. The data are presented as mean ± SEM. Statistical analysis was performed by paired t-test, chi-squared, ANOVA or Log-rank (Mantel-Cox) test as indicated in the figure legends and text. Results were considered significant when $P \leq 0.05$. All graphs were generated using GraphPad Prism software (version 8).

Acknowledgments

The results shown here are in part based upon data generated by the TCGA Research Network: https://www.cancer.gov/tcga. We thank Hao Ji and Dr Michael Shtutman form the UofSC Functional Genomics Core for the RNA sequencing analysis and Dr Vitali Sikirzhytski for help with fluorescent imaging. This study was supported by NSF (Award Number: OIA1736150).

Author disclosures. None exist

Supplementary Material:

Figure 1-Supplement Figure 1. Microsphere morphology of a panel of human lung cancer cells cultured in P. californicus sera.

Figure 3-Supplement Figure 1. CSC markers in A549 cells cultured in vitro and tumors

Figure 3-Supplement Figure 2. Unsupervised hierarchical clustering based on log2 transformed values on all RNAseq data.

Figure 3-Supplement Figure 3. RNA seq analysis summary of A549 cells.

Figure 4-Supplement Figure 1. Microsphere morphology of A549 human lung cancer cells cultured in P. maniculatus or P. polionotus sera.

References

1. Aizer AA, Chen MH, McCarthy EP, et al. Marital status and survival in patients with cancer. J Clin Oncol. 2013;31(31):3869-3876. doi:10.1200/JCO.2013.49.6489
2. Elwert F, Christakis NA. The effect of widowhood on mortality by the causes of death of both spouses. Am J Public Health. 2008;98(11):2092–2098. doi:10.2105/AJPH.2007.114348
3. Blanner, C., Mejldal, A., Prina, A., Munk-Jørgensen, P., Ersbøll, A., & Andersen, K. (2020). Widowhood and mortality: A Danish nationwide register-based cohort study. Epidemiology and Psychiatric Sciences, 29, E149. doi:10.1017/S2045796020000591.
4. Allison R. Sullivan, Andrew Fenelon, Patterns of Widowhood Mortality, The Journals of Gerontology: Series B, Volume 69B, Issue 1, January 2014, Pages 53–62, https://doi.org/10.1093/geronb/gbt079
5. Bowling A. (1987). Mortality after bereavement: A review of the literature on survival periods and factors affecting survival. Social Science & Medicine, 24, 117–124. doi:10.1016/0277-9536(87)90244-9
6. Boyle, P. J., Feng, Z., & Raab, G. M. (2011). Does Widowhood Increase Mortality Risk? Epidemiology, 22(1), 1-5. doi:10.1097/ede.0b013e3181fdcc0b
7. Burgoa M, Regidor E, Rodriguez C, Gutierrez-Fisac JL. Mortality by cause of death and marital status in Spain. Eur J Public Health 1998;8:37–42
8. Martikainen P, Valkonen T. Mortality after the death of a spouse: rates and causes of death in a large Finnish cohort. Am J Public Health 1996;86:1087–1093
9. Gove WR. Sex, marital status mortality. AJS 1973;79:45–67
10. Sullivan AR, Fenelon A. Patterns of widowhood mortality. J Gerontol B Psychol Sci Soc Sci. 2014;69(1):53-62. doi:10.1093/geronb/gbt079

11. Helsing KJ, Szklo M, Comstock GW. Factors associated with mortality after widowhood. Am J Public Health. 1981;71(8):802-809. doi:10.2105/ajph.71.8.802
12. Kleiman DG. Monogamy in mammals. Q Rev Biol. 1977 Mar;52(1):39-69. doi: 10.1086/409721. PMID: 857268
13. D. Lukas, T. H. Clutton-Brock, The evolution of social monogamy in mammals. Science 341, 526-530 (2013).
14. Scribner JL, Vance EA, Protter DSW, Sheeran WM, Saslow E, Cameron RT, Klein EM, Jimenez JC, Kheirbek MA, Donaldson ZR. A neuronal signature for monogamous reunion. Proc Natl Acad Sci U S A. 2020 May 19;117(20):11076-11084. doi: 10.1073/pnas.1917287117. Epub 2020 May 7. PMID: 32381740; PMCID: PMC7245077.
15. Chatzistamou I, Farmaki E, Kaza V, Kiaris H. The Value of Outbred Rodent Models in Cancer Research. Trends Cancer. 2018 Jul;4(7):468-471. doi: 10.1016/j.trecan.2018.05.004.
16. McDonald PG, Antoni MH, Lutgendorf SK, et al. A biobehavioral perspective of tumor biology. Discov Med. 2005;5(30):520-526.
17. Ben-Shaanan TL, Schiller M, Azulay-Debby H, Korin B, Boshnak N, Koren T, Krot M, Shakya J, Rahat MA, Hakim F, Rolls A. Modulation of anti-tumor immunity by the brain's reward system. Nat Commun. 2018 Jul 13;9(1):2723. doi: 10.1038/s41467-018-05283-5
18. Sloan EK, Priceman SJ, Cox BF, et al. The sympathetic nervous system induces a metastatic switch in primary breast cancer. Cancer Res. 2010;70(18):7042-7052. doi:10.1158/0008-5472.CAN-10-0522
19. Havighorst A, Crossland J, Kiaris H. Peromyscus as a model of human disease. Semin Cell Dev Biol. 2017 Jan; 61:150-155. doi: 10.1016/j.semcdb.2016.06.020.

20. Perea-Rodriguez JP, Takahashi EY, Amador TM, Hao RC, Saltzman W, Trainor BC.Effects of reproductive experience on central expression of progesterone, oestrogen α, oxytocin and vasopressin receptor mRNA in male California mice (Peromyscus californicus). J Neuroendocrinol. 2015 Apr;27(4):245-52. doi: 10.1111/jne.12264.
21. Wright EC, Parks TV, Alexander JO, Supra R, Trainor BC. Activation of kappa opioid receptors in the dorsal raphe have sex dependent effects on social behavior in California mice. Behav Brain Res. 2018 Oct 1;351:83-92. doi: 10.1016/j.bbr.2018.05.011. Epub 2018 Jun 7. Erratum in: Behav Brain Res.
22. Glasper ER, Devries AC. Social structure influences effects of pair-housing on wound healing. Brain Behav Immun. 2005 Jan;19(1):61-8. doi: 10.1016/j.bbi.2004.03.002. PMID: 15581739.
23. Fingert HJ, Treiman A, Pardee AB. Transplantation of human or rodent tumors into cyclosporine-treated mice: a feasible model for studies of tumor biology and chemotherapy. Proc Natl Acad Sci U S A. 1984;81(24):7927-7931. doi:10.1073/pnas.81.24.7927
24. Kaza V, Farmaki E, Havighorst A, Crossland J, Chatzistamou I, Kiaris H. Growth of human breast cancers in Peromyscus. Dis Model Mech. 2018;11(1):dmm031302. Published 2018 Jan 17. doi:10.1242/dmm.031302.
25. Chatzistamou I, Kiaris H. Modeling estrogen receptor-positive breast cancers in mice: is it the best we can do? Endocr Relat Cancer. 2016 Nov;23(11):C9-C12. doi: 10.1530/ERC-16-0397. Epub 2016 Sep 12. PMID: 27619257; PMCID: PMC5063077.
26. Visvader JE, Lindeman GJ. Cancer stem cells: current status and evolving complexities. Cell Stem Cell. 2012;10(6):717-728. doi:10.1016/j.stem.2012.05.007

27. Ishiguro T, Ohata H, Sato A, Yamawaki K, Enomoto T, Okamoto K. Tumor-derived spheroids: Relevance to cancer stem cells and clinical applications. Cancer Sci. 2017;108(3):283-289. doi:10.1111/cas.13155

28. Chiou SH, Wang ML, Chou YT, et al. Coexpression of Oct4 and Nanog enhances malignancy in lung adenocarcinoma by inducing cancer stem cell-like properties and epithelial-mesenchymal transdifferentiation. Cancer Res. 2010;70(24):10433-10444. doi:10.1158/0008-5472.CAN-10-2638

29. Akunuru, S., James Zhai, Q. & Zheng, Y. Non-small cell lung cancer stem/progenitor cells are enriched in multiple distinct phenotypic subpopulations and exhibit plasticity. Cell Death Dis 3, e352 (2012). https://doi.org/10.1038/cddis.2012.93

30. Teng Y, Wang X, Wang Y, Ma D. Wnt/beta-catenin signaling regulates cancer stem cells in lung cancer A549 cells. Biochem Biophys Res Commun. 2010;392(3):373-379. doi:10.1016/j.bbrc.2010.01.028

31. Vidman L, Källberg D, Rydén P. Cluster analysis on high dimensional RNA-seq data with applications to cancer research - An evaluation study. PLoS One. 2019 Dec 5;14(12):e0219102. doi: 10.1371/journal.pone.0219102. PMID: 31805048; PMCID: PMC6894875.

32. Ge, S.X., Son, E.W. & Yao, R. iDEP: an integrated web application for differential expression and pathway analysis of RNA-Seq data. BMC Bioinformatics 19, 534 (2018). https://doi.org/10.1186/s12859-018-2486-6

33. Westhoff B, Colaluca IN, D'Ario G, Donzelli M, Tosoni D, Volorio S, Pelosi G, Spaggiari L, Mazzarol G, Viale G, Pece S, Di Fiore PP. Alterations of the Notch pathway in lung cancer.

Proc Natl Acad Sci U S A. 2009 Dec 29;106(52):22293-8. doi: 10.1073/pnas.0907781106. Epub 2009 Dec 10. PMID: 20007775; PMCID: PMC2799768.

34. Yuan, X., Wu, H., Xu, H. et al. Meta-analysis reveals the correlation of Notch signaling with non-small cell lung cancer progression and prognosis. Sci Rep 5, 10338 (2015). https://doi.org/10.1038/srep10338
35. Zhu B, Yang JR, Jia Y, et al. Overexpression of NR4A1 is associated with tumor recurrence and poor survival in non-small-cell lung carcinoma. Oncotarget. 2017;8(69):113977-113986. Published 2017 Dec 8. doi:10.18632/oncotarget.23048
36. Hedrick E, Mohankumar K, Safe S. TGFβ-Induced Lung Cancer Cell Migration Is NR4A1-Dependent. Mol Cancer Res. 2018 Dec;16(12):1991-2002. doi: 10.1158/1541-7786.MCR-18-0366. Epub 2018 Aug 2. PMID: 30072581; PMCID: PMC6343492.
37. He B.,You L., Uematsu K., Zang K., Xu Z., Lee A.Y., Costello J.F., McCormick F., Jablons D.M. SOCS-3 is frequently silenced by hypermethylation and suppresses cell growth in human lung cancer., Proc Natl Acad Sci U S A. 2003; 100: 14133-14138.
38. Lund PK, Rigby RJ. SOC-ing it to tumors: suppressors of cytokine signaling as tumor repressors. Gastroenterology. 2006 Jul;131(1):317-9. doi: 10.1053/j.gastro.2006.05.030. PMID: 16831614.
39. Sahni A, Simpson-Haidaris PJ, Sahni SK, Vaday GG, Francis CW. Fibrinogen synthesized by cancer cells augments the proliferative effect of fibroblast growth factor-2 (FGF-2). J Thromb Haemost. 2008 Jan;6(1):176-83. doi: 10.1111/j.1538-7836.2007.02808.x. Epub 2007 Oct 22. PMID: 17949478.

40. Zhang X, Wang F, Huang Y, et al. FGG promotes migration and invasion in hepatocellular carcinoma cells through activating epithelial to mesenchymal transition. Cancer Manag Res. 2019;11:1653-1665. Published 2019 Feb 19. doi:10.2147/CMAR.S188248
41. Pieters M, Wolberg AS. Fibrinogen and fibrin: An illustrated review. Res Pract Thromb Haemost. 2019 Mar 4;3(2):161-172. doi: 10.1002/rth2.12191. PMID: 31011700; PMCID: PMC6462751.
42. Shimizu Y, Kinoshita I, Kikuchi J, Yamazaki K, Nishimura M, Birrer MJ, Dosaka-Akita H. Growth inhibition of non-small cell lung cancer cells by AP-1 blockade using a cJun dominant-negative mutant. Br J Cancer. 2008 Mar 11;98(5):915-22. doi: 10.1038/sj.bjc.6604267. Epub 2008 Feb 19. PMID: 18283312; PMCID: PMC2266861.
43. Chien W, Yin D, Gui D, Mori A, Frank JM, Said J, Kusuanco D, Marchevsky A, McKenna R, Koeffler HP. Suppression of cell proliferation and signaling transduction by connective tissue growth factor in non-small cell lung cancer cells. Mol Cancer Res. 2006 Aug;4(8):591-8. doi: 10.1158/1541-7786.MCR-06-0029. PMID: 16877704.
44. Chang CC, Shih JY, Jeng YM, Su JL, Lin BZ, Chen ST, Chau YP, Yang PC, Kuo ML. Connective tissue growth factor and its role in lung adenocarcinoma invasion and metastasis. J Natl Cancer Inst. 2004 Mar 3;96(5):364-75. doi: 10.1093/jnci/djh059. Erratum in: J Natl Cancer Inst. 2018 Jun 1;110(6):683. PMID: 14996858.
45. Jašarević E, Bailey DH, Crossland JP, Dawson WD, Szalai G, Ellersieck MR, Rosenfeld CS, Geary DC. Evolution of monogamy, paternal investment, and female life history in Peromyscus. J Comp Psychol. 2013 Feb;127(1):91-102. doi: 10.1037/a0027936. Epub 2012 Apr 30. PMID: 22545763.

46. Lutgendorf SK, Sood AK, Anderson B, et al. Social support, psychological distress, and natural killer cell activity in ovarian cancer. J Clin Oncol. 2005;23(28):7105-7113. doi:10.1200/JCO.2005.10.015

47. Fagundes CP, Bennett JM, Derry HM, Kiecolt-Glaser JK. Relationships and Inflammation across the Lifespan: Social Developmental Pathways to Disease. Soc Personal Psychol Compass. 2011;5(11):891-903. doi:10.1111/j.1751-9004.2011.00392.x

48. Fuligni AJ, Telzer EH, Bower J, Cole SW, Kiang L, Irwin MRA preliminary study of daily interpersonal stress and C-reactive protein levels among adolescents from Latin American and European backgrounds. Psychosom Med. 2009 Apr; 71(3):329-33

49. Yuan, L., Liu, S., Bai, X. M., Gao, Y., Liu, G. H., Wang, X. E., et al. (2016). Oxytocin inhibits lipopolysaccharide-induced inflammation in microglial cells and attenuates microglial activation in lipopolysaccharide-treated mice. *J. Neuroinflamm.* 13:7. doi: 10.1186/s12974-016-0541-7

50. Carter CS, Perkeybile AM. The Monogamy Paradox: What Do Love and Sex Have to Do With It?. *Front Ecol Evol*. 2018;6:202. doi:10.3389/fevo.2018.00202

51. Matarazzo V, Schaller F, Nédélec E, Benani A, Pénicaud L, Muscatelli F, Moyse E, Bauer S. Inactivation of Socs3 in the hypothalamus enhances the hindbrain response to endogenous satiety signals via oxytocin signaling. J Neurosci. 2012 Nov 28;32(48):17097-107. doi: 10.1523/JNEUROSCI.1669-12.2012. PMID: 23197703

52. Chavez B, Farmaki E, Zhang Y, Altomare D, Hao J, Soltnamohammadi E, Shtutman M, Chatzistamou I, & Kiaris H. A strategy for the Identification of Paracrine Regulators of Cancer Cell Migration. Clin Exp Pharmacol Physiol. 2020 Jun 25. doi: 10.1111/1440-1681.13366

Table 1. Differentially expressed genes between the B, BD and V groups. Chromosomal location, fold change (log2) and adjusted P value are indicated. Genes that are common in the B vs BD and V vs B comparisons are underlined.

Symbol	Chr	log2 Fold Change	Adj.Pval
BD vs B			
FGG	4q32.1	1.49	8.82e-04
FGA	4q31.3	1.37	8.82e-04
FGB	4q31.3	1.24	2.78e-03
HES1	3q29	1.16	3.36e-06
NR4A1	12q13.13	1.13	1.42e-09
SOCS3	17q25.3	1.09	4.39e-10
ZFP36	19q13.2	1.02	1.77e-03
V vs B			
CTGF	6q23.2	1.26	5.68e-02
HES1	3q29	1.18	2.26e-06
ZFP36	19q13.2	1.16	9.80e-05
NR4A1	12q13.13	1.12	3.41e-09
FGG	4q32.1	1.08	5.39e-02
JUN	1p32.1	1.04	3.36e-02
SOCS3	17q25.3	1.04	3.54e-09

Table 2. Biological processes associated with the differentially expressed genes in B vs BD and V vs B groups (37). The adjusted P values are indicated.

Group comparison	adj.Pval	Biological Process
BD vs B	3.1e-06	Positive regulation of substrate adhesion-dependent cell spreading
V vs B	4.9e-04	Blood vessel development
	5.3e-04	Positive regulation of intracellular signal transduction
	5.3e-04	Anatomical structure morphogenesis
	5.3e-04	Regulation of cellular protein metabolic process
	5.3e-04	Negative regulation of apoptotic process
	5.3e-04	Positive regulation of cell differentiation
	5.3e-04	Regulation of epithelial cell proliferation

Figure legends

Figure 1. **Effects of pair bonding in the pro-oncogenic activity of sera. a**. Representative microphotographs of tumor spheroids developed by A549 cells 3 days after cell seeding. Cells formed spheroids in the presence of sera from bonded (B), bond-disrupted animals (BD) 1 week after disruption, and virgin animals (V), and control media containing FBS (CM). Live (green) and dead cells (red) are indicated. Representative images of 2 independent experiments are shown. **b**. Representative microphotographs of tumor spheroids developed by A549 cells on day 1, day 2, and day 3, after cell seeding. Cells formed spheroids in the presence of sera from bonded (B), bond-disrupted animals (BD) 24h, 1 week, and 2 weeks after disruption, and virgin animals (V), control media containing FBS (CM) or serum-free plain media (PM). The last column shows images at day 3 in higher magnification. Bars indicate 200 μM. **c**. Scatter dot plots of data shown in (b) indicating the size of tumor spheroids at day 2 and 3 after seeding. Median and P values are indicated. Sera from 9 (B), 5 (BD, 24h), 5 (BD, 1wk), 4 BD (2wk) and 5(V) different animals were used and microsphere formation was evaluated in 2 biological replicas for each (n=10 for BD (1wk), BD (24h) and v; n=8 for BD (2wks) and n=18 for B). For control media (CM) and plain serum free media (PM) n=4. For this experiment sera from 14-17 months old mice were used that for the B and BD groups were bonded for about 1 year. Statistical analyses were performed by ANOVA.

Figure 2. **Growth of A549 human lung cancers in *P. californicus* (IS stock) and bonding experience.** Vasectomized males were used in all studies. **a**. Volume of measurable tumors at day 15 following cancer cell inoculation in the bonded (n=9), bond disrupted (n=8), and virgin (n=6) groups, out of the 11, 9 and 8 animals implanted originally with A549 cells. **b.** Pie graphs

indicating the percentage of animals bearing tumors at day 25. **c.** Representative H&E stained sections of P. *californicus*-grown tumors from bonded (upper panel), and bond disrupted (lower panel) groups. (*) and (#) indicate necrotic areas and muscle invasion, respectively. **d.** Tumor free nude mice implanted with A549 tumor explants from bonded (n=9) and bond-disrupted (n=7) *P. californicus*. P values (Log-rank (Mantel-Cox) test) are shown. **e.** H&E-stained sections of A549 tumors in nude mice derived from explants of A549 tumors from bonded, and bond-disrupted *P. californicus*. The morphology of A549 tumors from the direct inoculation of A549 cells in nude mice is shown (n). N is indicated in the text. B-IS, tumors growing in bonded P. californicus; BD-IS, tumors growing in bond-disrupted P. californicus; B-n, tumors that originally developed in bonded P. californicus and now growing in nude mice; BD-n, tumors that originally developed in bond-disrupted P. californicus and now growing in nude mice; n, tumors that developed in nude mice following injection of A549 cells.

Figure 3. **RNA seq analysis of A549 cells cultured in the presence of sera from bonded (B), bond-disrupted (BD) or virgin (V) P. californicus. a.** Bar graphs showing number of differentially expressed genes in each pairwise comparison group. **b**. Volcano plots showing differentially expressed genes between the B vs BD, and B vs V groups. **c.** Venn Diagrams showing overlapping differentially expressed genes. The identity of genes is shown in the right. In the bonded group, mice were paired for 12 months. For the bond-disrupted group, we separated paired mice after 12 months of bonding, and collected the sera one week after bond-disruption. For virgin mice, we collected sera from mice housed 3/cage.

Figure 4. Tumor spheroids with sera from P. polionotus and P. maniculatus. Morphology of tumor spheroids formed after 2, 3, and 7 days in culture with sera isolated from monogamous P. polionotus and polygamous P. maniculatus. In 6 out of 12 P. polionotus but none of 12 P. maniculatus enhanced dispersion was noted at bond disruption. For the experiment, sera were obtained from the same animal at bonding for 12 months and after 1 week following bond disruption. Bond-disrupted animals were housed independently after separation from females. BW B, P. maniculatus bonded; BW BD, P. maniculatus bond-disrupted; PO B, P. polionotus bonded; PO BD, P. polionotus bond disrupted

Figure 1

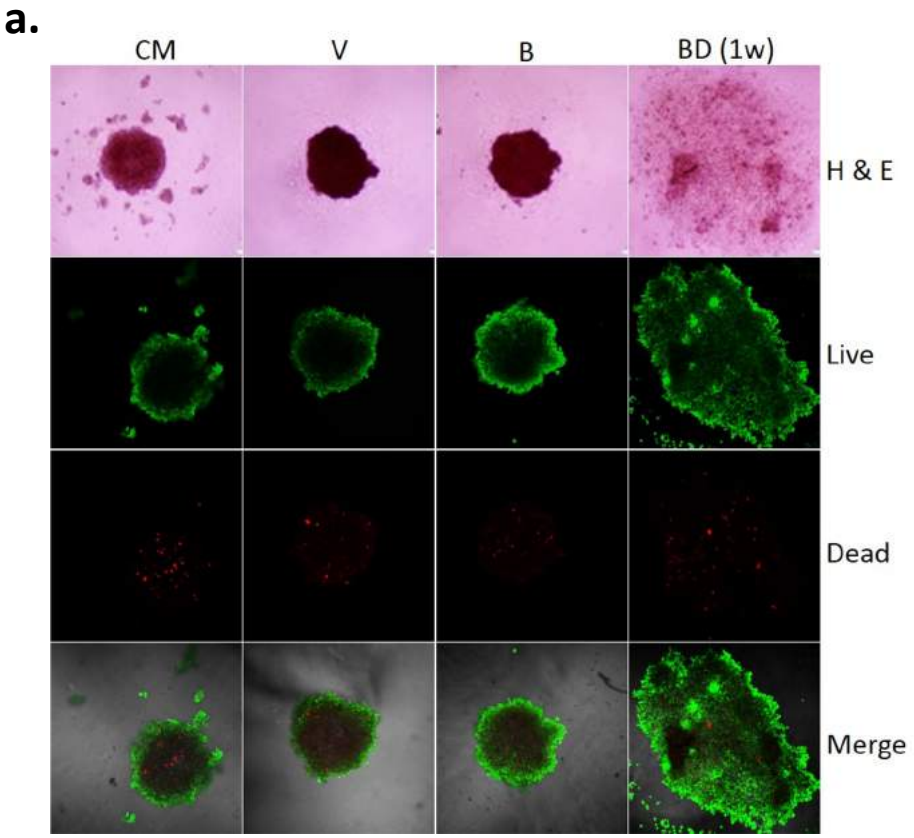
a.
CM
V
B
BD (1w)
H & E
Live
Dead
Merge

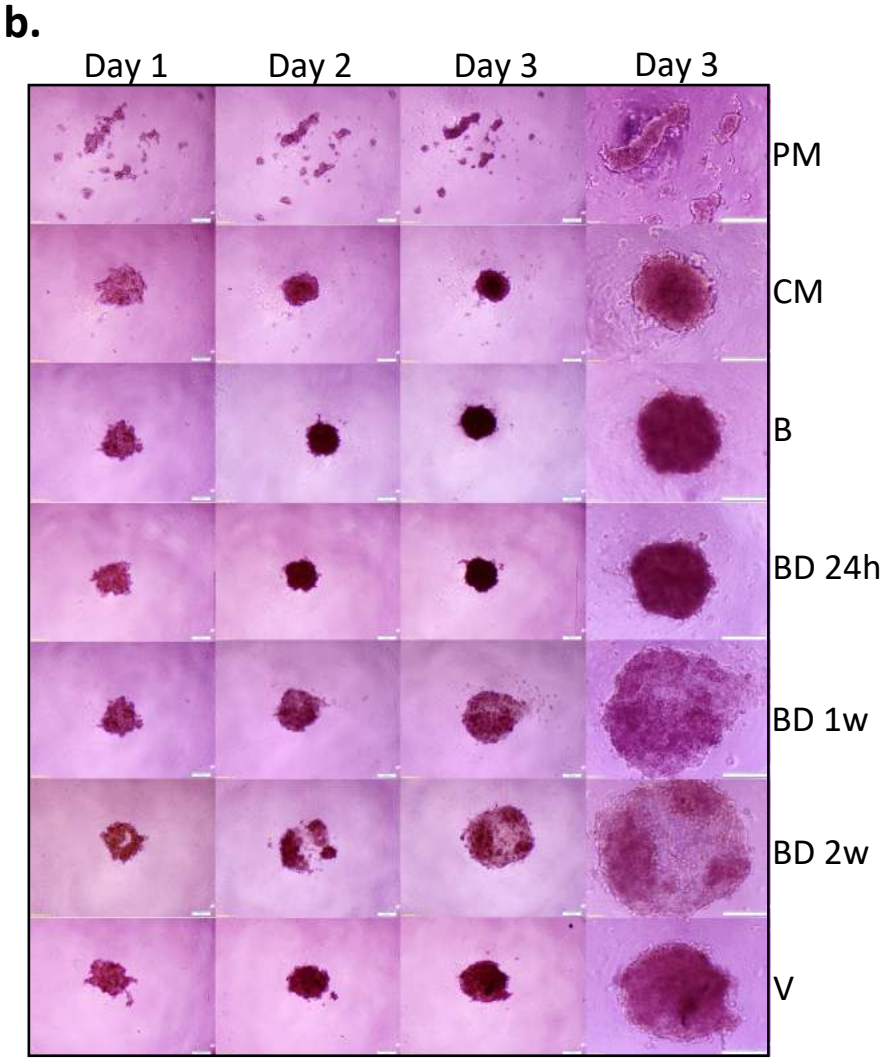
b.
Day 1
Day 2
Day 3
Day 3
PM
CM
B
BD 24h
BD 1w
BD 2w
V

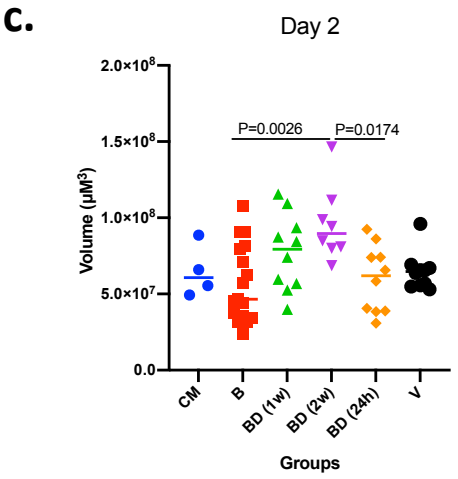
c.
Day 2
P=0.0026
P=0.0174
Volume (μM³)
2.0×10⁸
1.5×10⁸
1.0×10⁸
5.0×10⁷
0.0
CM
B
BD (1w)
BD (2w)
BD (24h)
V
Groups

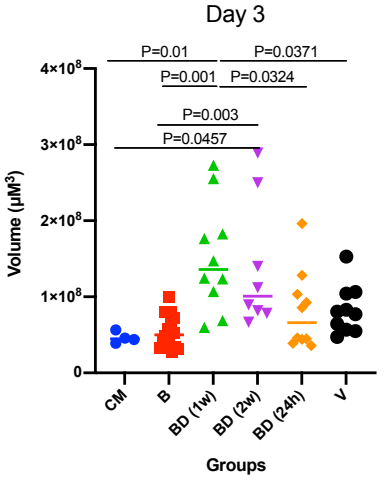
Day 3
P=0.01
P=0.0371
P=0.001
P=0.0324
P=0.003
P=0.0457
Volume (μM³)
4×10⁸
3×10⁸
2×10⁸
1×10⁸
0
CM
B
BD (1w)
BD (2w)
BD (24h)
V
Groups

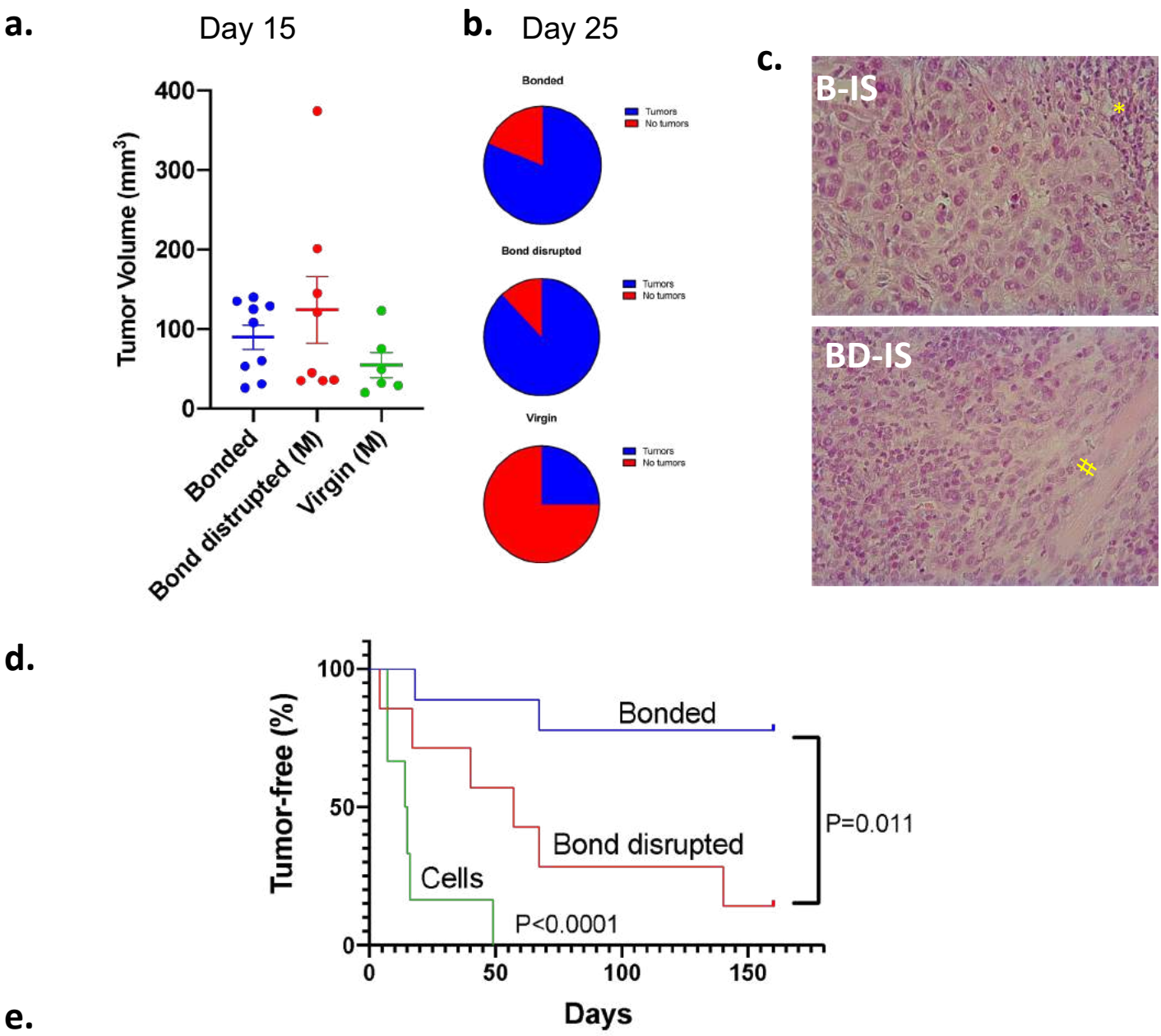
a.
Day 15
Tumor Volume (mm3)
400
300
200
100
0
Bonded
Bond distrupted (M)
Virgin (M)
b.
Day 25
Bonded
Tumors
No tumors
Bond disrupted
Tumors
No tumors
Virgin
Tumors
No tumors
c.
B-IS
BD-IS
d.
Tumor-free (%)
100
50
0
Bonded
Bond disrupted
Cells
P=0.011
P<0.0001
0
50
100
150
Days
e.
B-n
BD-n
n

Figure 2

a

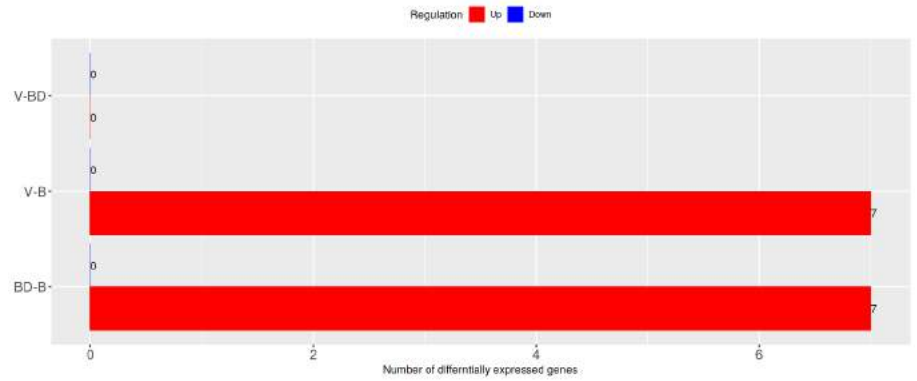

b

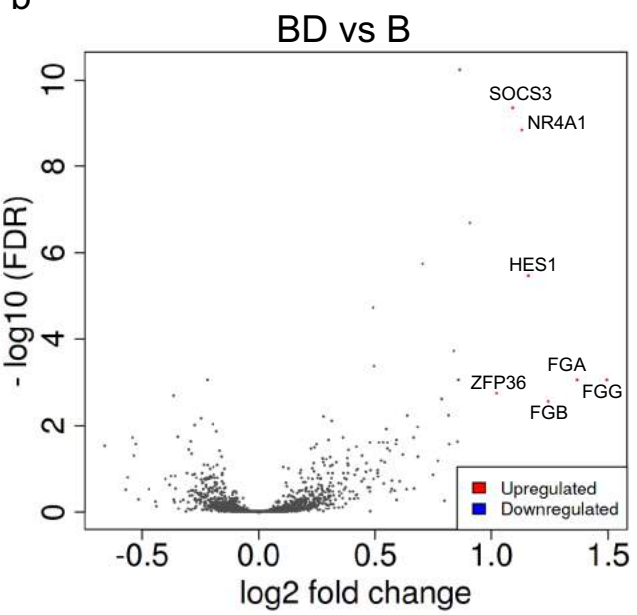

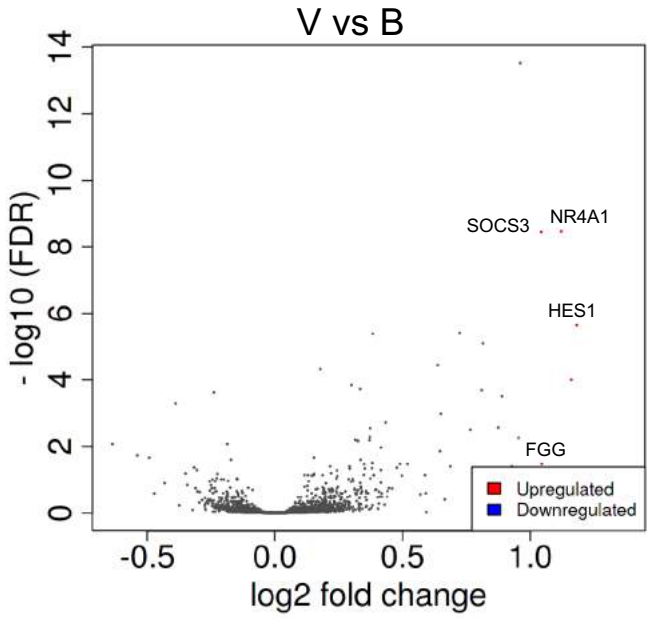

c

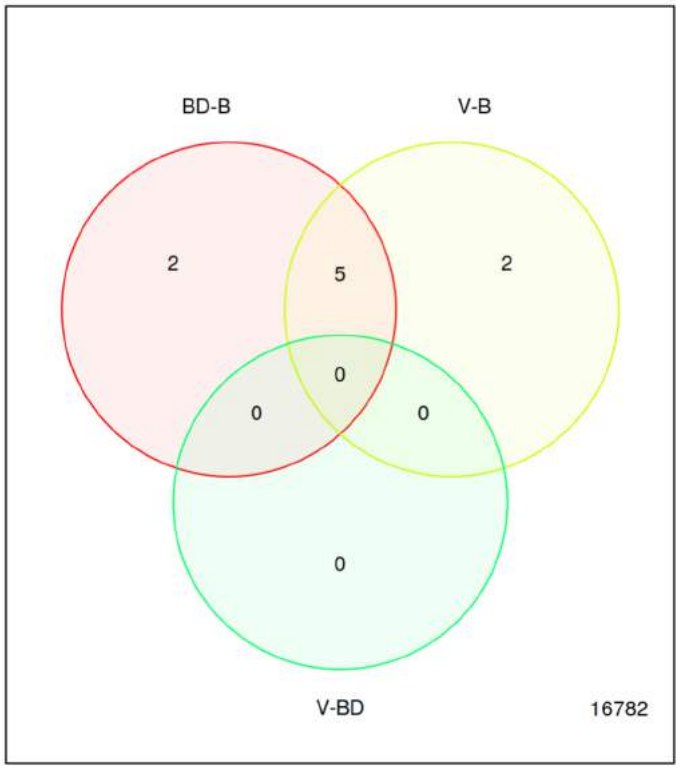

BD vs B & V vs B

HES1
ZFP36
NR4A1
FGG
SOCS3

BD vs B

FGA
FGB

V vs B

CTFG
JUN

Figure 3

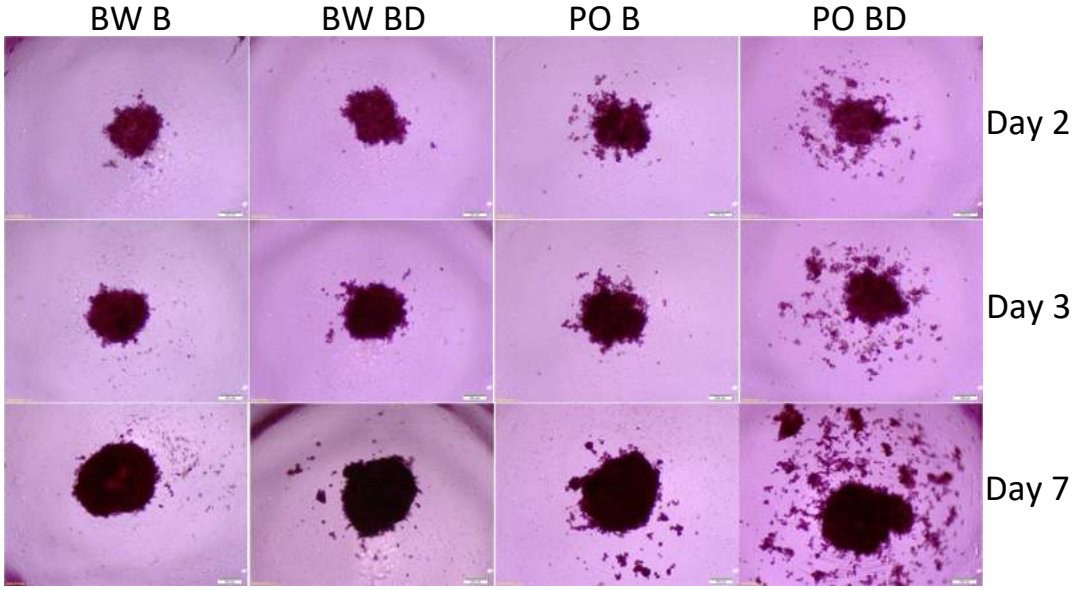

Figure 4

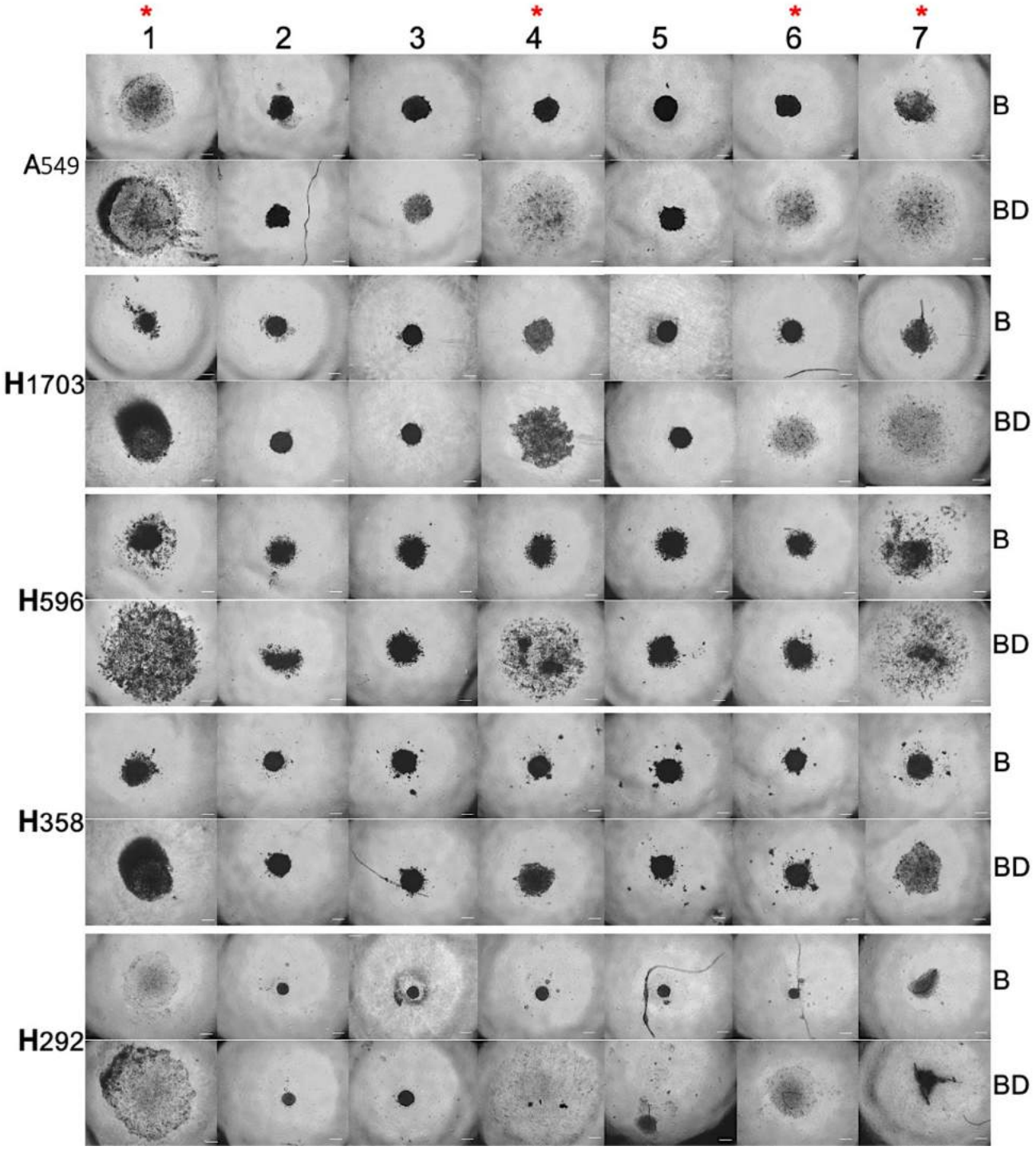

Figure 1-Supplementary Figure 1. Microsphere morphology of a panel of human lung cancer cells cultured for 3 days (A549) or 6 days (H1703, H596, H358, H292) with sera from 8-10 months old P. californicus, that were either pair bonded (B) for 2 months or following 2 weeks of bond disruption (BD) after 2 months of bonding. Sibling pairs were used that are shown in the upper and lower panel for each cell line. Asterisks in the top of sibling pair numbers indicate those at which consistently for all cell lines enhancement of spheroid size was noted. Bars indicate 200 µM.

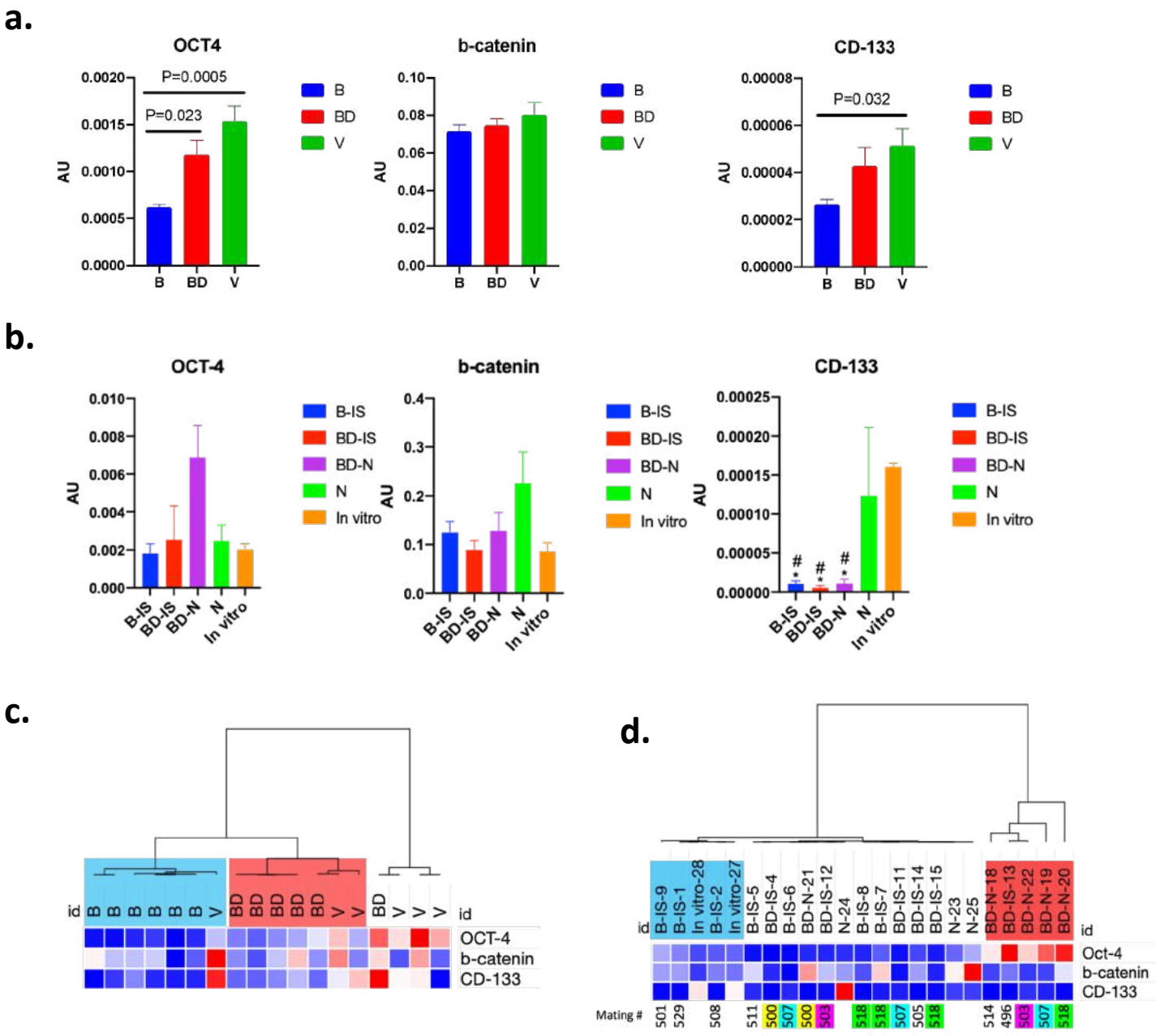

Figure 3-Figure Supplement 1. CSC markers in A549 cells cultured in vitro and tumors. a. Expression of OCT-4, CD-133, and b-catenin, evaluated by semi-quantitative RT-PCR, in A549 cells cultured in the presence of sera from bonded (B), bond-disrupted (BD), and virgin animals (V). Data are expressed as means ± SEM. N=6. P values are indicated (ANOVA). **b.** Expression of Oct-4, CD-133, and b-catenin, in tumors grown in P. californicus that are either bonded (B-IS), bond-disrupted (BD-IS), or implanted subsequently in nude mice following their growth in bond disrupted (BD-N) P. californicus. Cells cultured in vitro or tumors in nude mice without prior exposure to P. californicus were also included. *, P<0.05 vs N, #, P<0.05 vs in vitro; (ANOVA). Data are expressed as means ± SEM. N=7 (B-IS), =6 (BD-IS), or =5 (BD-N). **c.** Hierarchical clustering of A549 cells cultured in the presence of sera from bonded (B, blue highlight), bond-disrupted (BD, red highlight), and virgin animals (V), in relation to the expression of Oct-4, CD-133, and b-catenin. **d.** Hierarchical clustering of A549 tumors in relation to the expression of Oct-4, CD-133, and b-catenin. Individual tumors are indicated according to their original host's ID. The three branches consist exclusively of tumors from bond-disrupted animals (red highlight), tumors from both bonded and bond-disrupted animals (no highlight), and tumors from bonded animals (blue highlight) are shown. Mating # indicating siblings are indicated and highlighted with the same color. Tumors from nude mice (N) without prior exposure to P. californicus were also included in this analysis. For this experiment in the bonded group, mice were paired for at least 2 months before the study began and remained paired until the end of the study. In the bond-disrupted group, mice were paired 2 months before the study started, and immediately after cancer cells injection, they were separated. In the virgin group, mice were kept individually 2 months before the study began.

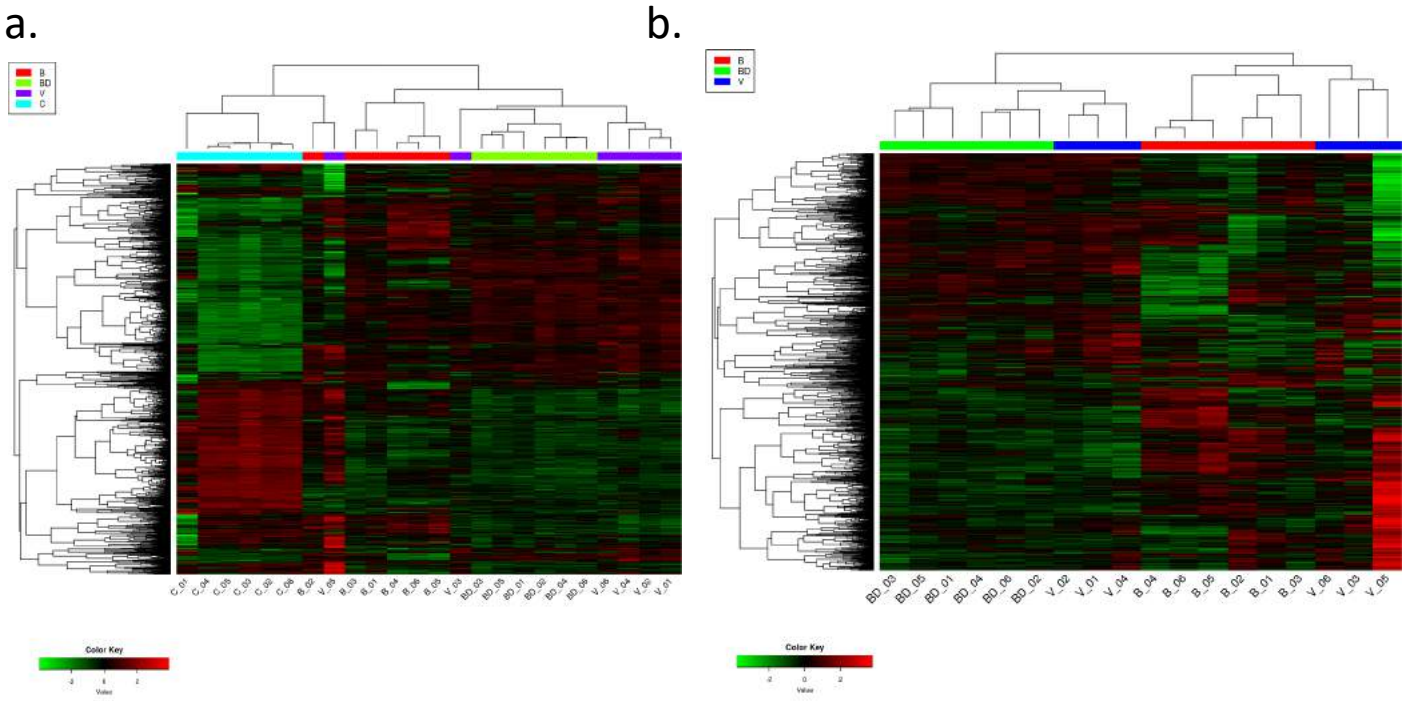

Figure 3-Figure Supplement 2. Hierarchical clustering of RNA seq data. In (a), all 4 groups were included while in (b), only specimens cultured with Peromyscus sera were included. For these analyses 2,000 most variable genes were used. The analysis was performed by using the iDEP.91 platform (http://bioinformatics.sdstate.edu/idep/).

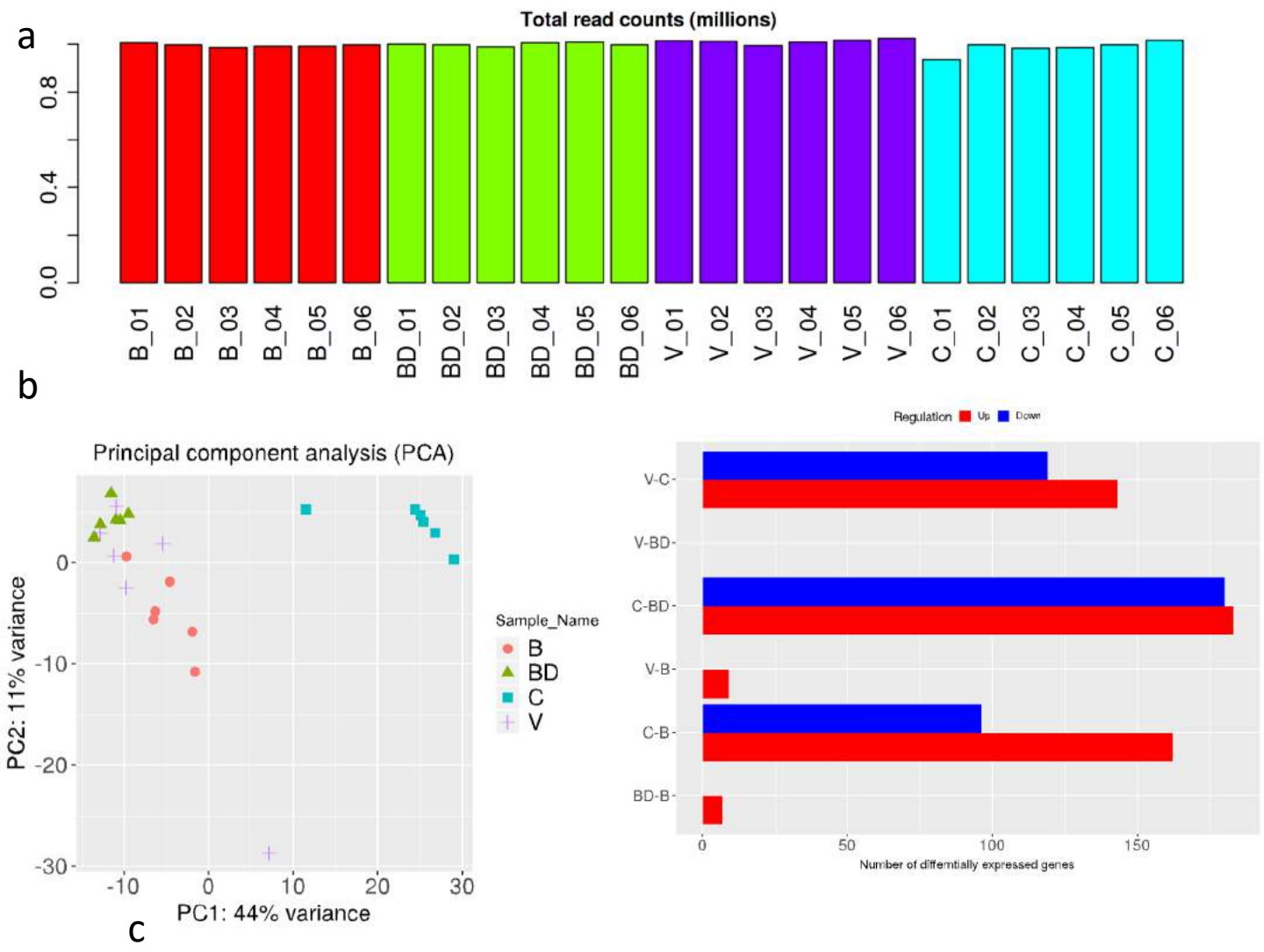

Figure - Figure Supplement 3. RNA seq analysis of A549 cells cultured in the presence of sera from bonded (B), bond disrupted (BD) and virgin (V) P. californicus. FBS grown cells were also included (C). A. RNA seq reads, b. Principal component analysis of RNA seq data. C. Number of differentially expressed genes in all pairwise comparisons.

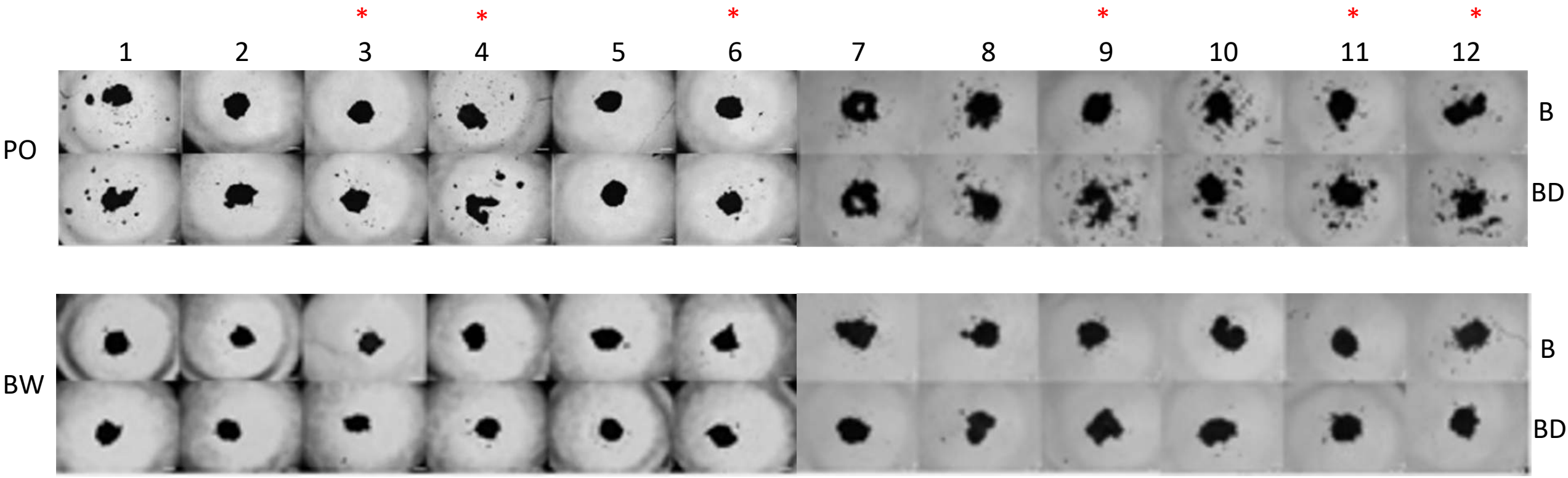

Figure 4-Figure Supplement 1. Microsphere morphology of A549 human lung cancer cells cultured for 3 days with sera from 14-30 months old P. polionotus (PO) or 12-21 months old P. maniculatus (BW), that were pair bonded (B) for about 12 months or following 1 week of bond disruption (BD). For this experiment sera from the same animals at bonding and bond disruption were used. Asterisks in the top indicate those animals at which enhanced dispersion of spheroids (scattered phenotype) was noted after bond disruption (in 6 out of 12 for PO vs . 0 out of 12 for BW; P=0.005, chi-square test). For all samples microsphere formation assay were done in duplicate and the results for both replicate were always consistent. In some instances (for example #1 and #8), a "scattered" spheroid morphology in PO was seen at bonding as well. For this, qualitative assessment of the spheroids, the "scattered" phenotype was scored when at least 2 outgrowths formed distal from the main spheroid.